Impurity modes from impurity clusters in photonic band structures

1995 J. Phys.: Condens. Matter 7 447

(http://iopscience.iop.org/0953-8984/7/2/022)

J. Phys.: Condens. Matter 7 (1995) 447–462. Printed in the UK

Impurity modes from impurity clusters in photonic band structures

H G Algul†, M Khazhinsky†, A R McGurn† and J Kapenga‡

† Department of Physics, Western Michigan University, Kalamazoo, MI 49008, USA

‡ Department of Computer Science, Western Michigan University, Kalamazoo, MI 49008, USA

Received 31 May 1994, in final form 13 September 1994

Abstract. A Green function calculation for the impurity modes of single impurities and clusters of impurities in a photonic band structure is given. Specifically, a truncated two-dimensional periodic dielectric medium composed from a square lattice array of dielectric rods placed perpendicularly between two parallel perfectly conducting plates is studied. Impurities are introduced into this system substitutionally by replacing one (single impurity case) or a number (cluster impurity case) of the rods in the periodic system by impurity rods. Exact expressions for the impurity mode frequencies are obtained in terms of the Green functions of the pure system. These expressions are then evaluated for the case of impurities with small cross-sectional areas using numerically determined Green functions. Linear frequency-independent, linear frequency-dependent and non-linear impurity dielectric media are treated.

1. Introduction

Recently there has been much interest in the study of electromagnetic bands associated with the propagation of electromagnetic waves in periodic dielectric media [1–8]. A number of papers on the computation of such photonic band structures have appeared, dealing with waves propagating in 3D, 2D and 1D periodic dielectric arrays. While early computations only treated media formed from frequency-independent materials with positive dielectric constants [1–7], more recent efforts have addressed systems of frequency-dependent dielectric materials that can exhibit negative dielectric constants [8, 9].

The original interest in photonic band structures arose from their possible use in suppressing spontaneous atomic emissions, which often are a mechanism of energy loss in solid-state and laser systems [6]. More recent interest in photonic band structures has centred on the use of impurity modes in these systems to develop new types of lasers [6, 10]. A number of papers have appeared on the computation of impurity levels in 3D, 2D and 1D systems [10–14]. These works generally regard the computation for single size or dielectric impurities in otherwise periodic media. All the systems considered of which we are aware have dealt solely with linear frequency-independent dielectric media.

In this paper we consider the Green function computation of impurity levels in a 2D truncated photonic band structure [15, 16]. Specifically, a periodic array of dielectric rods with circular cross sections is bounded between two parallel perfectly conducting plates that cut the rods perpendicular to their axes. This is then the model for a periodic array in a waveguide. A single impurity rod or cluster of impurity rods is introduced substitutionally into the system and an exact expression for the impurity mode frequencies is obtained in terms of Green functions for the pure system. The impurity mode frequencies as functions of

0953-8984/95/020447+16$19.50

the parameters characterizing the impurity are then obtained using numerically determined values of the Green functions. In these considerations linear frequency-independent, linear frequency-dependent and non-linear dielectric impurities will be treated.

The Green function techniques that we use are quite standard [17–21]. These methods have been previously applied first in the study of impurity modes in electron conduction and lattice vibration systems, and more recently to the study of single magnetic impurities in magnetic systems. The generalization to treat impurity levels in photonic systems is straightforward.

The order of this paper is as follows. In section 2, we discuss the Green function solution of our impurity model and obtain an exact equation, the solutions of which yield the impurity frequency modes. In section 3 we discuss the numerical evaluation of our equation for the impurity frequency modes. In section 4, our conclusions are given.

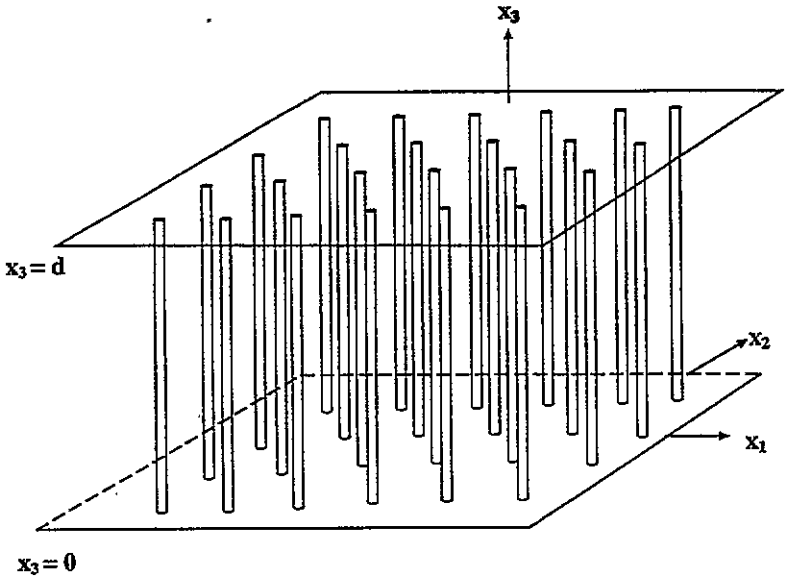

Figure 1. The waveguide configuration.

2. Green function theory

The system we consider (see figure 1) consists of an infinite square lattice array of parallel dielectric rods characterized by a dielectric constant ϵ_a, embedded in a background medium whose dielectric constant is ϵ_b. The rods will be of circular cross section with radius R and the lattice constant of the square lattice is a, with $a > 2R$. The resulting spatially inhomogeneous dielectric medium fills the region between two parallel perfectly conducting plates at $x_3 = 0$ and $x_3 = d$ such that the parallel plates are perpendicular to the axes of the rods [15]. (The rods are then periodically arrayed in the x_1x_2 plane such that the axes of the rods occur at $(x_1, x_2) = (na, ma)$, where n and m are integers.) An impurity is added substitutionally to this system by changing one or a cluster of rods in the system [11].

In the absence of an impurity, the modes of the parallel-plate waveguide system were solved for in [15]. In [15] it was shown that for

$$\boldsymbol{E}(x;t) = \boldsymbol{E}(x|\omega)\exp(-\mathrm{i}\omega t) \tag{1}$$

one obtains

$$E_1(x|\omega) = \sum_{G_\parallel}\sum_{n=1}^{\infty} a_1^{(n)}(k_\parallel + G_\parallel)\exp[\mathrm{i}(k_\parallel + G_\parallel)\cdot x_\parallel]\sin\left(\frac{n\pi x_3}{d}\right) \tag{2a}$$

$$E_2(x|\omega) = \sum_{G_\parallel}\sum_{n=1}^{\infty} a_2^{(n)}(k_\parallel + G_\parallel)\exp[\mathrm{i}(k_\parallel + G_\parallel)\cdot x_\parallel]\sin\left(\frac{n\pi x_3}{d}\right) \tag{2b}$$

$$E_3(x|\omega) = \mathrm{i}\sum_{G_\parallel}\sum_{n=0}^{\infty} \epsilon_n a_3^{(n)}(k_\parallel + G_\parallel)\exp[\mathrm{i}(k_\parallel + G_\parallel)\cdot x_\parallel]\cos\left(\frac{n\pi x_3}{d}\right) \tag{2c}$$

where $\epsilon_0 = 1/2$ and $\epsilon_n = 1$ for $n \geqslant 1$. Here the $a_\alpha^{(n)}(k_\parallel + G_\parallel)$ are solutions of

$$\sum_{G'_\parallel}\hat{k}(G_\parallel - G'_\parallel)\{[(k_2+G'_2)^2 + (n\pi/d)^2]a_1^{(n)}(k_\parallel + G'_\parallel) - (k_1+G'_1)(k_2+G'_2)a_2^{(n)}(k_\parallel + G'_\parallel)$$

$$+ (k_1+G'_1)(n\pi/d)a_3^{(n)}(k_\parallel + G'_\parallel)\} = (\omega^2/c^2)a_1^{(n)}(k_\parallel + G_\parallel) \tag{3a}$$

$$\sum_{G'_\parallel}\hat{k}(G_\parallel - G'_\parallel)\{-(k_2+G'_2)(k_1+G'_1)a_1^{(n)}(k_\parallel+G_\parallel) + [(k_1+G'_1)^2 + (n\pi/d)^2]a_2^{(n)}(k_\parallel+G'_\parallel)$$

$$+ (k_2+G'_2)(n\pi/d)a_3^{(n)}(k_\parallel + G'_\parallel)\} = (\omega^2/c^2)a_2^{(n)}(k_\parallel + G_\parallel) \tag{3b}$$

$$\sum_{G'_\parallel}\hat{k}(G_\parallel - G'_\parallel)[(k_1+G'_1)(n\pi/d)a_1^{(n)}(k_\parallel + G'_\parallel) + (k_2+G'_2)(n\pi/d)a_2^{(n)}(k_\parallel + G'_\parallel)$$

$$+ (k_\parallel + G'_\parallel)^2 a_3^{(n)}(k_\parallel + G'_\parallel)] = (\omega^2/c^2)a_3^{(n)}(k_\parallel + G_\parallel) \tag{3c}$$

with

$$\hat{k}(G_\parallel) = \begin{cases} (1/\epsilon_a)f + (1/\epsilon_b)(1-f) & G_\parallel = 0 \quad (4a) \\ (1/\epsilon_a - 1/\epsilon_b)f2J_1(G_\parallel R)/(G_\parallel R) & G_\parallel \neq 0. \quad (4b) \end{cases}$$

Here R is the radius of the rods; $f = \pi R^2/a^2$ is the filling fraction, i.e. the fraction of the total volume of the structure occupied by the rods, where a is the lattice parameter; and $J_1(x)$ is a Bessel function.

Equations (3) constitute a standard eigenvalue problem for the electromagnetic modes in the waveguide [15] and was solved in [15] for the band structures of the modes labelled respectively $n = 0$, 1 and 2.

From Maxwell's equations we find the following wave equation for the waveguide in the presence of a dielectric impurity [11]:

$$\left(\mathsf{L} - \frac{\omega^2}{c^2}\right)\mathbf{E} = \frac{\delta\epsilon(x_\parallel)}{\epsilon_0(x_\parallel)}\frac{\omega^2}{c^2}\mathbf{E} \tag{5}$$

where

$$\mathbf{L} = \frac{1}{\epsilon_0(x_\parallel)} \begin{vmatrix} -\partial^2/\partial x_2^2 - \partial^2/\partial x_3^2 & \partial^2/\partial x_1 \partial x_2 & \partial^2/\partial x_1 \partial x_3 \\ \partial^2/\partial x_2 \partial x_1 & -\partial^2/\partial x_1^2 - \partial^2/\partial x_3^2 & \partial^2/\partial x_2 \partial x_3 \\ \partial^2/\partial x_3 \partial x_1 & \partial^2/\partial x_2 \partial x_3 & -\partial^2/\partial x_1^2 - \partial^2/\partial x_2^2 \end{vmatrix} \tag{6}$$

$$\mathbf{E} = \begin{vmatrix} E_1(x|\omega) \\ E_2(x|\omega) \\ E_3(x|\omega) \end{vmatrix} \tag{7}$$

$\epsilon_0(x_\parallel)$ is the position-dependent dielectric constant in the periodic system; and $\delta\epsilon(x_\parallel)$ is the change in the position-dependent dielectric constant, from that of the pure system, resulting from the addition of impurities. (We shall assume in the following that $\delta\epsilon(x_\parallel)$ is independent of x_3.) A formal solution for $\mathbf{E}$ in equation (5) can be easily expressed in terms of the electromagnetic modes of the waveguide in the absence of impurities. This solution follows from the orthonormality properties of the waveguide modes, which we shall now discuss.

If $\delta\epsilon(x_\parallel) = 0$ in (5), then

$$\epsilon_0(x_\parallel)\mathbf{L}\mathbf{E} = (\omega^2/c^2)\epsilon_0(x_\parallel)\mathbf{E} \tag{8}$$

defines a Sturm–Liouville eigenvalue problem for the Hermitian operator $\epsilon_0(x_\parallel)\mathbf{L}$. The eigenvectors $\mathbf{E}(x|\omega)$ of equation (8) can be labelled as states of $k_\parallel$ in the first Brillouin zone, r labelling the frequency band of the eigenvalue, and mode index n corresponding to the n in the arguments of the sine and cosine functions in (2), i.e.

$$\mathbf{E}^{(n)}_{rk_\parallel}(x|\omega) = \frac{1}{\sqrt{N^{(n)}_{rk_\parallel}}} \sum_{G_\parallel} \begin{pmatrix} a^{(n)}_{1r}(k_\parallel + G_\parallel)\sin[(n\pi/d)x_3] \\ a^{(n)}_{2r}(k_\parallel + G_\parallel)\sin[(n\pi/d)x_3] \\ \mathrm{i}\epsilon_n a^{(n)}_{3r}(k_\parallel + G_\parallel)\cos[(n\pi/d)x_3] \end{pmatrix} \exp[\mathrm{i}(k_\parallel + G_\parallel)\cdot x_\parallel]. \tag{9}$$

In equation (9)

$$N^{(n)}_{rk_\parallel} = \frac{d}{2}\sum_{G_\parallel}\sum_{G'_\parallel} \hat{\epsilon}(G'_\parallel - G_\parallel)[a^{(n)*}_{1r}(k_\parallel + G_\parallel)a^{(n)}_{1r}(k_\parallel + G'_\parallel) + a^{(n)*}_{2r}(k_\parallel + G_\parallel)a^{(n)}_{2r}(k_\parallel + G'_\parallel)$$
$$+ \epsilon_n^2 a^{(n)*}_{3r}(k_\parallel + G_\parallel)a^{(n)}_{3r}(k_\parallel + G'_\parallel)] \tag{10}$$

where $\hat{\epsilon}(G'_\parallel - G_\parallel)$ is the Fourier transform in $x_\parallel$ of $\epsilon_0(x_\parallel)$, and $\omega^2/c^2 = \lambda^{(n)}_{rk_\parallel}$ is the eigenvalue corresponding to the eigenvectors $a^{(n)}_{1r}(k_\parallel + G_\parallel)$, $a^{(n)}_{2r}(k_\parallel + G_\parallel)$, $a^{(n)}_{3r}(k_\parallel + G_\parallel)$ determined from equation (3). From equation (8) it then follows that the $\{E^{(n)}_{rk_\parallel}(x/\omega)\}$ are orthonormal such that

$$\int \mathrm{d}^3x\, \epsilon_0(x_\parallel)\mathbf{E}^{(n)+}_{sk_\parallel}\mathbf{E}^{(m)}_{rq_\parallel} = (2\pi)^2\delta(k_\parallel - q_\parallel)\delta_{n,m}\delta_{s,r}. \tag{11}$$

The electric field $\mathbf{E}$ in equation (5) can be expressed in terms of the orthonormal set $\{\mathbf{E}^{(n)}_{rk_\parallel}\}$ in equation (9) so that

$$\mathbf{E}(x) = \sum_r \sum_n \int \frac{\mathrm{d}^2k_\parallel}{(2\pi)^2} b^{(n)}_{rk_\parallel}\mathbf{E}^{(n)}_{rk_\parallel} \tag{12}$$

and substitution into equation (5) yields

$$b_r^{(n)}(k_\parallel) = \frac{\omega^2}{c^2} \frac{\int \mathrm{d}^3x\, \delta\epsilon(x_\parallel)\mathbf{E}_{rk_\parallel}^{(n)+}\mathbf{E}}{\lambda_{rk_\parallel}^{(n)} - \omega^2/c^2}. \tag{13}$$

From equations (12) and (13) we find that

$$\mathbf{E}(x) = \frac{\omega^2}{c^2} \int \mathrm{d}^3x'\, \delta\epsilon(x'_\parallel)\mathbf{G}(x|x')\mathbf{E}(x') \tag{14}$$

where

$$\mathbf{G}(x|x) = \sum_r \sum_n \int \frac{\mathrm{d}^2k_\parallel}{(2\pi)^2} \frac{\mathbf{E}_{rk_\parallel}^{(n)}(x)\mathbf{E}_{rk_\parallel}^{(n)+}(x')}{\lambda_{rk_\parallel}^{(n)} - \omega^2/c^2} \tag{15}$$

is the 3×3 matrix Green function. The impurity modes of the system are found as solutions of (14).

From equations (14) and (15) we see that for $\delta\epsilon(x_\parallel)$ independent of x_3 between the perfectly conducting plates, the impurity modes continue to be states of the $n = 0, 1, 2, \ldots$ waveguide mode indices. The index n remains a good label of the eigenmodes in the impure waveguide so that the band structures of each of the $n = 0, 1, \ldots$ modes can be studied separately and a determination of the impurity levels in the band of each mode can be made. For $\delta\epsilon(x)$ dependent on x_3, this simplification does not occur and the impurity mixes states of different n.

We shall now discuss the solution of equation (14) separately for modes of $n = 0$ and 1 for a number of interesting types of impurities. This will be followed in section 3 by the presentation of results of the numerical evaluation of equation (14) for these impurity types.

2.1. Cluster impurities

Let us consider introducing a cluster of cylindrical impurities of the form

$$\delta\epsilon(x_\parallel) = \delta\epsilon_0(x_\parallel) + \delta\epsilon_0(x_\parallel - a\hat{x}_1) + \delta\epsilon_0(x_\parallel + a\hat{x}_1) + \delta\epsilon_0(x_\parallel - a\hat{x}_2) + \delta\epsilon_0(x_\parallel + a\hat{x}_2) \tag{16}$$

where

$$\delta\epsilon_0(r) = \begin{cases} f(r) & \text{for } r < a/2 \\ 0 & \text{otherwise.} \end{cases} \tag{17}$$

This cluster transforms about $x_\parallel = 0$ under the same point group as that of the square lattice [21], and hence simple expressions for the impurity modes can be obtained using group theory methods.

Substituting equation (16) into equation (14) we find for $|x_\parallel| \leqslant r \ll a$

$$\epsilon(x) = \frac{\omega^2}{c^2} \int \mathrm{d}^3x'_\parallel\, \delta\epsilon_0(x'_\parallel)\mathbf{G}(x|x')\epsilon(x') \tag{18}$$

where $\epsilon(x)$ is a 15-component vector of the form

$$\begin{aligned}
&\epsilon_i(x) = E_i(x) \qquad i = 1, 2, 3 \\
&\epsilon_i(x) = E_{i-3}(x + a\hat{x}_1) \qquad i = 4, 5, 6 \\
&\epsilon_i(x) = E_{i-6}(x - a\hat{x}_1) \qquad i = 7, 8, 9 \\
&\epsilon_i(x) = E_{i-9}(x + a\hat{x}_2) \qquad i = 10, 11, 12 \\
&\epsilon_i(x) = E_{i-12}(x - a\hat{x}_2) \qquad i = 13, 14, 15
\end{aligned} \tag{19}$$

and

$$\mathbf{G}(x|x') = \begin{vmatrix} G_{00} & G_{01} & G_{01} & G_{01} & G_{01} \\ G_{01} & G_{00} & G_{12} & G_{13} & G_{13} \\ G_{01} & G_{12} & G_{00} & G_{13} & G_{13} \\ G_{01} & G_{13} & G_{13} & G_{00} & G_{12} \\ G_{01} & G_{13} & G_{13} & G_{12} & G_{00} \end{vmatrix} \tag{20}$$

where

$$G_{00} = \mathbf{G}(x|x') \tag{21a}$$

$$G_{01} = \mathbf{G}(x|x' + a\hat{x}_1) \tag{21b}$$

$$G_{12} = \mathbf{G}(x + a\hat{x}_1|x' - a\hat{x}_1) \tag{21c}$$

$$G_{13} = \mathbf{G}(x + a\hat{x}_1|x' + a\hat{x}_2). \tag{21d}$$

The impurity modes of this system are obtained as the solutions of

$$\int \mathrm{d}^3x' \,[\delta(x - x') - (\omega/c)^2 \delta\epsilon_0(x_\parallel)\mathbf{G}(x|x')]\mathbf{f}(x') = 0 \tag{22}$$

where

$$\mathbf{f}(x|\omega) = \begin{cases} \epsilon(x) & \text{for } |x_\parallel| \leqslant r \\ 0 & \text{otherwise.} \end{cases} \tag{23}$$

The matrix integrand in equation (22) can be put into block diagonal form by using the 15×15 unitary matrix [21]

$$\mathbf{u} = \begin{vmatrix} \mathbf{1} & \mathbf{0} & \mathbf{0} & \mathbf{0} & \mathbf{0} \\ \mathbf{0} & (1/2)\mathbf{1} & (1/\sqrt{2})\mathbf{1} & \mathbf{0} & (1/2)\mathbf{1} \\ \mathbf{0} & (1/2)\mathbf{1} & -(1/\sqrt{2})\mathbf{1} & \mathbf{0} & (1/2)\mathbf{1} \\ \mathbf{0} & (1/2)\mathbf{1} & \mathbf{0} & (1/\sqrt{2})\mathbf{1} & -(1/2)\mathbf{1} \\ \mathbf{0} & (1/2)\mathbf{1} & \mathbf{0} & -(1/\sqrt{2})\mathbf{1} & -(1/2)\mathbf{1} \end{vmatrix} \tag{24}$$

where $\mathbf{1}$ is a 3×3 unit matrix and $\mathbf{0}$ is a 3×3 zero matrix, such that

$$\begin{aligned}
&\int \mathrm{d}^3x' \,\mathbf{u}^+[\delta(x - x') - (\omega/c)^2 \delta\epsilon_0(x'_\parallel)\mathbf{G}(x|x')]\mathbf{u}\mathbf{u}^+\mathbf{f}(x') \\
&\quad = \int \mathrm{d}^3x' \,[\delta(x - x') - (\omega/c)^2 \delta\epsilon_0(x'_\parallel)\mathbf{u}^+\mathbf{G}(x|x')\mathbf{u}]\mathbf{u}^+\mathbf{f}(x') = 0.
\end{aligned} \tag{25}$$

We then find

$$\mathbf{u}^{+}\mathbf{G}(x|x')\mathbf{u} = \begin{vmatrix} G_{00} & 2G_{01} & 0 & 0 & 0 \\ 2G_{01} & G_{s} & 0 & 0 & 0 \\ 0 & 0 & G_{p} & 0 & 0 \\ 0 & 0 & 0 & G_{p} & 0 \\ 0 & 0 & 0 & 0 & G_{d} \end{vmatrix} \tag{26}$$

where

$$G_{s} = G_{00} + 2G_{13} + G_{12} \tag{27a}$$

$$G_{p} = G_{00} - G_{12} \tag{27b}$$

$$G_{d} = G_{00} - 2G_{13} + G_{12} \tag{27c}$$

and the matrix that gives the solvability condition

$$\delta(x - x') - (\omega/c)^2 \delta\epsilon(x'_{\parallel})\mathbf{u}^{+}G(x|x')\mathbf{u} \tag{28}$$

is block diagonalized into three 3×3 matrices and one 6×6 matrix. The integral equation in (25) can be discretized in x and x', and expressed as the linear matrix equation

$$\sum_{j}(\delta_{ij} - (\omega/c)^2 \omega_j \delta\epsilon_0(x_j)\mathbf{u}^{+}G(x_i|x_j)\mathbf{u})\mathbf{u}^{+}\mathbf{f}(x_j) = 0 \tag{29}$$

where $\{\omega_j\}$ are the weights used to express $\int \mathrm{d}^3x$ in terms of a sum, $\sum_j$. The solvability condition is then that the determinant of the matrix in equation (29) vanishes, and the frequencies ω at which this occurs are the modes of the impurity states.

If $\delta\epsilon_0(x_{\parallel})$ is independent of x_3, then (25) can be separated into a set of independent equations for each of the $n = 0, 1, 2, \ldots$ waveguide modes. The indices $n = 0, 1, 2, \ldots$ remain as good mode indices for the eigenmodes of the impurity system and equation (25) can be reduced to an integral only over the x_1x_2 plane. This greatly simplifies the computation for a given n of the impurity modes of the system.

2.2. *Single impurity*

For a single impurity $\delta\epsilon(x_{\parallel}) = \delta\epsilon_0(x_{\parallel})$, and equation (14) reduces to the 3×3 matrix equation

$$\epsilon(x) = (\omega^2/c^2) \int \mathrm{d}^3x' \, \delta\epsilon_0(x'_{\parallel})G_{00}(x|x')\epsilon(x') \tag{30}$$

where

$$\epsilon_i(x) = E_i(x) \qquad i = 1, 2, 3. \tag{31}$$

This equation cannot be reduced by group theory considerations but is already in its simplest form. Upon discretization, a matrix equation is obtained from (30), which yields the solvability condition and the frequencies of the impurity modes of the system. If $\delta\epsilon_0(x_{\parallel})$ is independent of x_3, then multiplying equation (30) by $\sin[(n\pi/d)x_3]$ and integrating over x_3 reduces (30) to a set of independent mode equations for $n = 0, 1, 2, \ldots$ modes. These resulting mode equations are easily discretized in the plane $x_{\parallel}$ and simplify the evaluation of the gap modes for each of the given $n = 0, 1, \ldots$ waveguide mode indices.

2.3. Computation of impurity modes

The evaluation of equation (25) for clusters and equation (30) for single impurities can be further facilitated by considering $\delta\epsilon_0(x_\parallel)$ of the form

$$\delta\epsilon_0(x_\parallel) = \Delta\epsilon_{00}(x_\parallel) \tag{32}$$

where $\epsilon_{00}(x_\parallel)$ is a general function of $x_\parallel$ and Δ is a constant independent of $x_\parallel$, and we shall concentrate in the work presented below on results for $\delta\epsilon_0(x_\parallel)$ of the form given in equation (32). Substituting $\delta\epsilon_0(x_\parallel)$ from (32) into (25), we obtain the eigenvalue problem

$$g(x) = \Delta \int d^3x' \, \mathbf{K}(x|x')g(x) \tag{33}$$

where $g(x) = u^+ f(x)$, $\mathbf{K}(x|x') = (\omega^2/c^2)\mathbf{u}^+\mathbf{G}(x|x')\mathbf{u}\epsilon_{00}(x'_\parallel)$ and Δ is the eigenvalue.

Similarly, substituting (32) into (30) yields

$$\epsilon(x) = \Delta \int d^3x' \, K(x|x')\epsilon(x') \tag{34}$$

where $K(x|x') = (\omega^2/c^2)G_{00}(x|x')\epsilon_{00}(x')$. Both equations (33) and (34) are Fredholm eigenvalue problems, which yield Δ as a function of the impurity mode frequency ω/c and can be easily discretized and solved numerically as matrix eigenvalue problems. In the following we shall consider three different forms for $\epsilon_{00}(x_\parallel)$:

$$\epsilon_{00}(x_\parallel) = \delta(x_\parallel) \tag{35a}$$

$$\epsilon_{00}(x_\parallel) = \exp(-|x_\parallel|^2/b^2)/(\pi b^2) \tag{35b}$$

and

$$\epsilon_{00}(x_\parallel) = \begin{cases} 1/4b^2 & |x_1|, |x_2| < b \\ 0 & \text{otherwise.} \end{cases} \tag{35c}$$

We shall use these to compute the impurity modes for $n = 0$ and $n = 1$ waveguide nodes.

2.3.1. Delta function form. A simplification occurs in the evaluation of equations (25) and (30) if we assume that $\delta\epsilon_0(x_\parallel) = \Delta\delta(x_\parallel)$. This would correspond to making impurities in our system by placing a thin ($R_{\text{impurity}} \to 0$) cylindrical pin of length d along the axes of some of the $R > 0$ dielectric rods of the periodic system. Once this limiting case is understood, it will facilitate the numerical evaluation of (25) and (30) for more general sized impurities. We shall consider these more general sized impurities further on in this paper and in more detail in a future publication.

(i) *Delta function form $n = 0$ modes.* An additional simplification occurs in equation (25) for the computation of the $n = 0$ cluster modes. For this case $E_1(x|\omega) = E_2(x|\omega) = 0$, and the 15 and 15×15 vector and matrices in (25) are reduced to the 5 and 5×5 vector and matrices formed from the terms associated with the non-zero $E_3(x|\omega)$. Substituting $\delta\epsilon_0(x_\parallel) = \Delta\delta(x_\parallel)$ in our cluster impurity problem (equation (25)) yields for $n = 0$:

$$\Delta = \frac{G_s + G_{s2} \pm [(G_s - G_{s2})^2 + 16G_{s1}^2]^{1/2}}{2(\omega^2/c^2)(G_sG_{s2} - 4G_{s1}^2)} \tag{36}$$

$$\Delta = [(\omega/c)^2 G_p]^{-1} \tag{37}$$

$$\Delta = [(\omega/c)^2 G_d]^{-1} \tag{38}$$

where

$$G_s = \sum_r \int \frac{d^2k_\parallel}{(2\pi)^2} G_r(k_\parallel) \tag{39a}$$

$$G_{s1} = \sum_r \int \frac{dk_\parallel^2}{(2\pi)^2} \gamma_k G_r(k_\parallel) \tag{39b}$$

$$G_{2s} = \sum_r \int \frac{d^2k_\parallel}{(2\pi)^2} (1 + 2V_k + \gamma_{2k}) G_r(k_\parallel) \tag{39c}$$

$$G_p = \sum_r \int \frac{d^2k_\parallel}{(2\pi)^2} (1 - \gamma_{2k}) G_r(k_\parallel) \tag{39d}$$

$$G_d = \sum_r \int \frac{d^2k_\parallel}{(2\pi)^2} (1 - 2V_k + \gamma_{2k}) G_r(k_\parallel) \tag{39e}$$

$$G_r(k_\parallel) = \frac{(E^{(0)}_{rk_\parallel})^*_3 (E^{(0)}_{rk_\parallel})_3}{\lambda^{(0)}_{rk_\parallel} - \omega^2/c^2} \tag{39f}$$

$$V_k = \cos(k_x a)\cos(k_u a) \tag{40a}$$

$$\gamma_k = \tfrac{1}{2}[\cos(k_x a) + \cos(k_y a)]. \tag{40b}$$

Equations (36)–(38) then yield the impurity strength Δ as a function of the impurity mode frequency ω for modes of s, p and d symmetry, respectively. The Green functions in equation (39) are evaluated numerically on the computer.

In the single impurity $n = 0$ case, $\delta\epsilon_0(x_\parallel) = \Delta\delta(x_\parallel)$ yields from equation (30) a single impurity mode at frequency ω for Δ given by

$$\Delta = [(\omega/c)^2 G_s]^{-1} \tag{41}$$

where G_s is defined in (39*a*). Again G_s is evaluated numerically on the computer.

The $n = 0$ modes can also be treated for Kerr non-linear impurities. In this case, for both cluster and single impurity computations, we take $\delta\epsilon_0(x_\parallel) = A[1 + \lambda|E_3(x_\parallel|\omega)|^2]\delta(x_\parallel)$. Proceeding as above, we find that the single impurity result is given by (41) with Δ replaced by $A[1 + \lambda|E_3(0|\omega)|^2]$. The interesting feature of the non-linear results is that the $\lambda|E_3|^2$ term allows for the impurity mode frequencies to be tuned by varying the electric field intensity. The cluster modes for non-linear impurities are not as easy to treat as the single impurity case because E_3 on the shell sites can differ from E_3 at the centre site. As a rough approximation one might approximate a solution of the non-linear cluster by replacing Δ on the left-hand sides of (36)–(38) by $A[1 + \lambda|E_3(0|\omega)|^2]$ and solving for A as an eigenvalue. A more satisfactory treatment would, however, require a self-consistent treatment of the impurity problem, which would allow the shell impurities to differ in dielectric constant from the centre site impurity.

(ii) *Delta function form $n > 0$ modes.* Substituting $\delta\epsilon_0(x_\parallel) = \Delta\delta(x)$ into equation (25) for the $n > 0$ modes we find that Δ as a function of the impurity mode frequency ω can be obtained from (33) as the matrix eigenvalue problem

$$\mathbf{K}(0|0)g(0) = (1/\Delta)g(0) \tag{42}$$

for clusters and from (34) as the matrix eigenvalue problem

$$K(0|0)\epsilon(0) = (1/\Delta)\epsilon(0) \tag{43}$$

for single impurities. The matrix in (42) is 15×15 whereas the matrix in (43) is 3×3. For a given impurity mode frequency ω used to evaluate $\mathbf{K}$ in (42) or K in (43), we then obtain from equation (42) 15 values of Δ, which give cluster impurity modes of various symmetries at these frequencies, and three values of Δ from equation (43), which give single impurity modes at frequency ω.

2.3.2. Gaussian and step function forms. For these cases, given in (35*b*) and (35*c*), we use Hermite and Gaussian quadrature, respectively, to discretize and solve (33) for cluster mode and (34) for single impurity mode cases. We shall see below that, as the area of the defect in the x_1x_2 plane increases, for a fixed impurity mode frequency ω, the number of eigenvalue solutions for Δ at ω tend to increase. The delta function impurity profile is found to give a minimum number of Δ solutions for a fixed ω. For the delta function cases Δ is a single-valued function of ω for each distinct symmetry mode.

3. Numerical evaluation

In this section we present numerical studies of the $n = 0$ and $n = 1$ impurity modes for the single impurity and cluster of impurities defined in (32) and (16), respectively. For these evaluations we have taken $\delta\epsilon_0(x_\parallel)$ to be of the form given in (32) and (35) and have looked at the three cases given in (35), i.e. delta function, Gaussian and step function.

We have taken the parameters used in [15] to characterize the system in the absence of impurities. Specifically, for this system $\epsilon_a = 9$, $\epsilon_b = 1$ and the filling fraction is $f = 0.4488$. The $n = 0$ mode solutions are independent of the plate separation, but for the $n = 1$ mode results, which depend on d, we have taken a plate separation $d/a = 0.5$. Our interest in these pure system parameters is that they correspond to those of a system that has recently been investigated experimentally.

In the numerical evaluation of (25) and (30) we have used 377 plane waves for the $n = 0$ results and 137 plane waves for the $n = 1$ results presented below. These are, respectively, the same number of plane waves used to study the system in [15]. In all of the results presented below, discretized versions of (25) and (30) were used to solve for Δ as a function of the impurity mode frequency ω in terms of a matrix eigenvalue problem for $1/\Delta$. Results are presented for $n = 0$ impurity modes in the two lowest band gaps ($0.248 \leqslant \omega a/2\pi c \leqslant 0.277$ and $0.414 \leqslant \omega a/2\pi c \leqslant 0.468$) and for $n = 1$ impurity modes in the lowest band gap ($0.00 \leqslant \omega a/2\pi c \leqslant 0.44$).

In the following we shall first present results for delta function impurities for $n = 0$ solutions. These will be followed by results for the Gaussian and step function cases for $n = 0$ solutions. Finally $n = 1$ solution results will be presented for the delta function single impurity case.

3.1. Delta function form

We have evaluated (36)–(39) for the cluster impurity and (41) for the single impurity $n = 0$ cases. For the cluster impurity case results are presented for two s symmetry modes labelled s0 and s1, respectively, two degenerate p symmetry modes labelled p, and one d symmetry

mode labelled d. The result for the single impurity case is a single mode of s symmetry, labelled s.

In figure 2 we present results in the second lowest band gap $0.414 \leqslant \omega a/2\pi c \leqslant 0.468$ for the s0, s1, p and d symmetry cluster modes. The s1, p and d symmetry modes have values of Δ that are positive whereas the s0 modes have Δ that are negative. In all cases the absolute value of Δ is seen to decrease with increasing frequency ω. The single impurity mode results for this gap are presented in figure 3 and are found to exhibit Δ values very close to those for the p and d symmetry modes in the cluster impurity case.

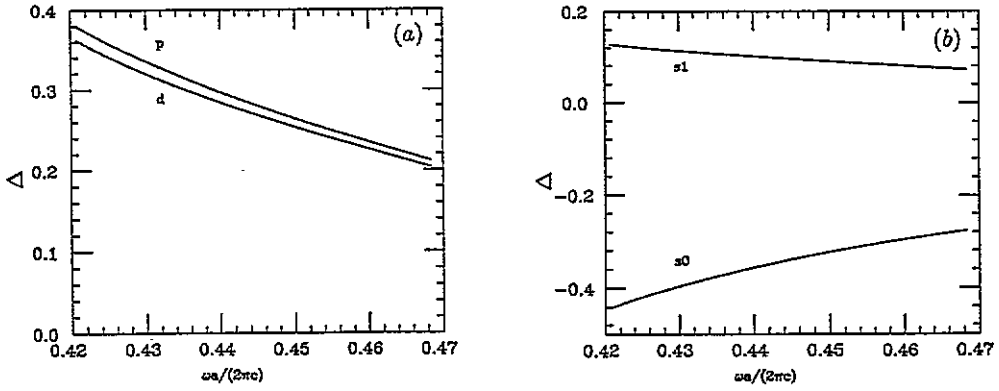

Figure 2. Plot of Δ versus impurity mode frequency ω in the second band gap for (a) p and d symmetry modes and (b) s0 and s1 symmetry modes. These results are obtained for the form given in (35a).

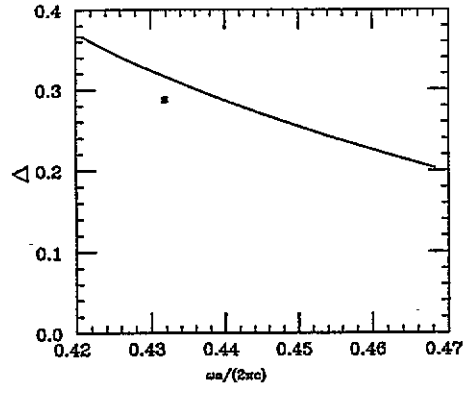

Figure 3. Plot of Δ versus impurity mode frequency ω in the second band gap for the single site impurity. The results are obtained for the form given in (35a).

An interesting feature of the single impurity results in figure 3 is that, for a given impurity mode frequency ω, there is only one value of Δ giving a mode at ω. This is different from the behaviour of Δ on ω that we shall see below for the Gaussian and step function impurities. In general, we find that, as the cross-sectional area of the impurity increases in the x_1x_2 plane from zero, Δ becomes a multiple-valued function of impurity mode frequency ω. For the cluster impurity results in figure 2, again Δ for the s0, s1, p and

d modes are single-valued functions of impurity mode frequencies and these each become multiple-valued functions of ω as the cross-sectional area of the impurity is increased.

In figures 4 and 5 we present results in the lowest band gap $0.248 \leqslant \omega a/2\pi c \leqslant 0.277$ for the s0, s1, p and d symmetry cluster modes and the s symmetry single impurity modes. Again, the p and d cluster modes exhibit a similar functional dependence of Δ on ω. The s0 and s1 cluster modes and the s single impurity modes, however, both exhibit a rather interesting functional dependence of Δ on ω. The s single impurity forms for Δ exhibit an asymptote at which there is an abrupt sign change in Δ as a function of ω, and the s0 and s1 cluster modes exhibit a minimum and maximum, respectively, in the dependence of Δ on ω. All of the forms for Δ (i.e. s, s0, s1, p, d), however, exhibit a single-valued dependence on ω.

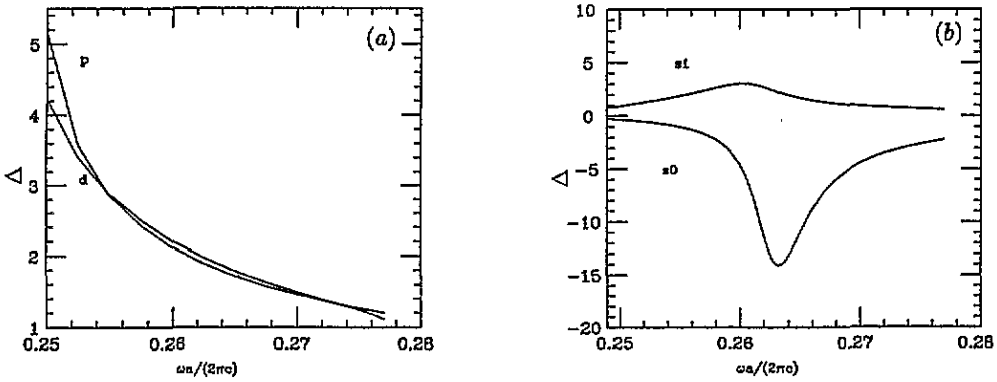

Figure 4. Plot of Δ versus impurity mode frequency ω in the lowest band gap for (a) cluster impurity modes of p and d symmetry and (b) cluster impurity mode of s0 and s1 symmetry. These results are obtained for the form given in (35a).

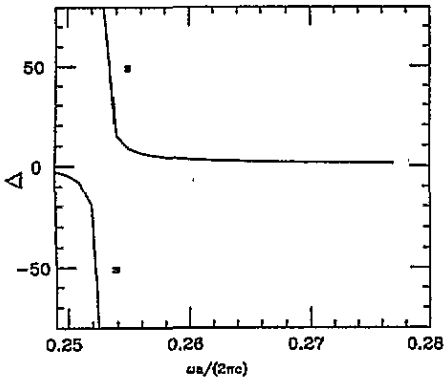

Figure 5. Plot of Δ versus impurity mode frequency ω in the lowest band gap for the single site impurity. The results are obtained for the form given in (35a).

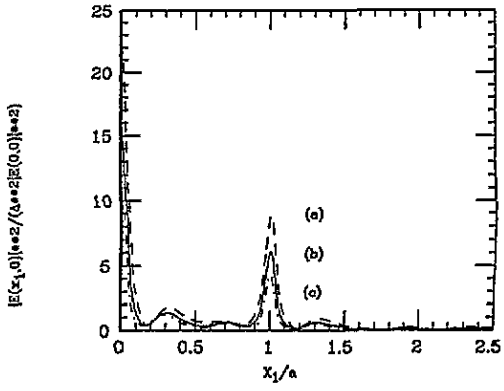

Figure 6. Plot of $|E(x_1, 0)|^2$ versus x_1 for localized single impurity modes of frequencies (a) $\omega a/2\pi c = 0.465$, (b) $\omega a/2\pi c = 0.450$ and (c) $\omega a/2\pi c = 0.435$.

Equation (14) can be used to determine the electric field in space of the impurity modes. In figure 6 we present results for $|E(x_1, 0)|^2$ versus x_1 for single impurity $n = 0$ modes. A number of impurity mode solutions with different mode frequencies in the second lowest band gap are shown. In general, the modes are found to be localized about the site of the impurity and the sites of nearest-neighbour rods. The half-width of the central peak about the impurity is approximately $0.05a$ for each frequency. Figure 7 presents similar results for $|E(x_1, 0)|^2$ versus x_1 for single impurity $n = 0$ mode frequencies in the lowest band gap. In these cases we see that $|E|^2$ is small at the impurity site but is still localized in the vicinity of the impurity.

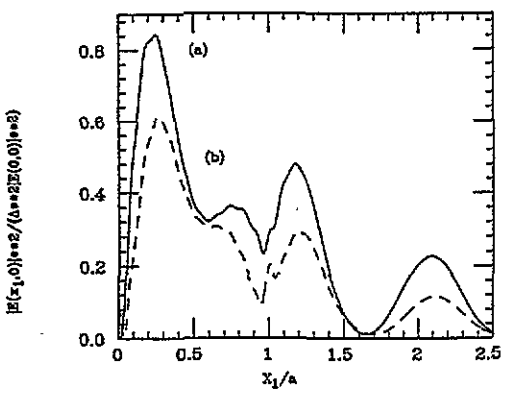

Figure 7. Plot of $|E(x_1, 0)|^2$ versus x_1 for localized single impurity modes of frequencies (*a*) $\omega a/2\pi c = 0.253$ and (*b*) $\omega a/2\pi c = 0.260$.

3.2. Gaussian function and step function form $n = 0$ results

We have evaluated the $n = 0$ impurity modes using the Gaussian form in (35*b*) with $b = 0.01a$. The integral equations in (33) and (34) are discretized in $x_\parallel$ using Hermite quadrature and yield matrix eigenvalue problems for the eigenvalues Δ^{-1}. For the 2D integral in $x_\parallel$ we have used 25-point 2D Hermite quadrature, yielding a 25×25 matrix eigenvalue problem with multiple solutions for Δ at a given impurity mode frequency ω.

In table 1 we present the three smallest values of Δ for the single impurity $n = 0$ mode and the p and d cluster modes for a number of impurity mode frequencies in the second lowest frequency gap. In addition, results for the single impurity mode in the lowest frequency gap are also presented. In general, we see that one value of Δ for each of the above modes is shifted below the single values of Δ given in section 3.1 for the delta function form. This is not surprising in light of the dependence of $|E|^2$ on x_1 seen in figures 6 and 7 for the delta function form.

We have also evaluated the $n = 0$ impurity modes using the step function form in (35*c*) with $b = 0.01a$. The integral equations in (33) and (34) are discretized using Gaussian quadrature and yield matrix eigenvalue problems for the eigenvalue Δ^{-1}. For the 2D integral in $x_\parallel$ we have used 25-point 2D Gaussian quadrature, yielding a 25×25 matrix with multiple solutions for Δ at a given impurity mode frequency ω.

In table 2 we present step function results for the three smallest values of Δ for the single impurity mode, and the p and d cluster modes for a number of impurity mode frequencies in the second frequency gap. Additional single impurity mode results are also presented for frequencies in the lowest frequency gap. These results are found to be similar to those from the Gaussian profile.

Table 1. Impurity strength Δ as a function of ω: Gaussian data.

$\omega a/2\pi c$	0.425	0.430	0.435	0.440	0.445	0.450	0.455	0.460
s	0.362	0.339	0.318	0.299	0.282	0.265	0.249	0 234
	18.0	17.2	16.5	16.0	15.5	15.0	14.6	14.2
	18.1	17.3	16.6	16.0	15.5	15.0	14.6	14.2
p	0.375	0.351	0.330	0.310	0.292	0.275	0.259	0.244
	17.7	17.0	16.4	15.9	15.4	14.9	14.5	14.1
	17.8	17.1	16.5	15.9	15.4	15.0	14.5	14.1
d	0.357	0.334	0.314	0.296	0.279	0.263	0.248	0.234
	18.7	17.6	16.8	16.2	15.6	15.1	14.7	14.2
	18.9	17.7	16.9	16.2	15.6	15.2	14.7	14.3

$\omega a/2\pi c$	0.2500	0.2525	0.2550	0.2575	0.2600	0.2625	0.2650	0.2675
s	−3.62	−14.1	−178.2	5.75	3.90	3.03	2.52	2.17
	45.0	40.8	12.8	43.3	42.3	41.4	40.5	39.6
	46.2	45.2	44.2	45.3	43.7	42.5	41.5	40.5

Table 2. Impurity strength Δ as a function of ω: step function data.

$\omega a/2\pi c$	0.425	0.430	0.435	0.440	0.445	0.450	0.455	0.460
s	0.357	0.334	0.313	0.295	0.278	0.262	0.246	0.232
	25.3	24.1	23.3	22.5	21.8	21.1	20.6	20.0
	25.5	24.3	23.4	22.5	21.9	21.1	20.6	20.0
p	0.369	0.346	0.325	0.306	0.288	0.271	0.256	0.241
	24.8	23.9	23.2	22.4	21.8	21.1	20.5	20.0
	24.9	24.1	23.2	22.4	21.8	21.1	20.5	20.0
d	0.351	0.330	0.309	0.292	0.276	0.261	0.246	0.232
	26.2	24.7	23.7	22.8	22.0	21.3	20.6	20.1
	26.5	25.0	23.8	22.9	22.0	21.4	20.8	20.1

$\omega a/2\pi c$	0.2500	0.2525	0.2550	0.2575	0.2600	0.2625	0.2650	0.2675
s	−3.83	−19.4	11.6	5.37	3.71	2.90	2.43	2.10
	63.8	56.3	62.6	61.2	60.0	58.7	57.4	56.1
	65.3	57.4	69.0	63.9	61.8	60.1	58.7	57.3

3.3. Delta function for $n = 1$ results

We have evaluated the single impurity delta function results for $n = 1$. The matrix eigenvalue problem in (43) yields three values of Δ for each impurity mode frequency ω. Results for the lowest $n = 1$ band gap $0.00 \leqslant \omega a/2\pi c \leqslant 0.44$ are presented in table 3. In general the three Δ are seen to be decreasing functions of ω and two values of Δ at fixed ω are seen to be almost degenerate. The three Δ solutions at fixed ω correspond to three modes of different electric field polarizations.

4. Conclusions

We have used Green function techniques to compute the impurity modes in photonic band

Table 3. Impurity strength Δ as a function of ω: delta function data.

$\omega a/2\pi c$	0.1	0.18	0.26	0.34	0.42
	13.9	4.16	1.83	0.84	0.25
	15.0	4.34	1.84	0.84	0.25
	15.1	4.38	1.91	1.02	0.58

structures. Both single impurity and cluster impurity cases were considered, and it is found that the numerical computational efforts for single and cluster impurities are the same.

By treating impurities for which $\delta\epsilon_0(x_\parallel)$ is of the form $\delta\epsilon_0(x_\parallel) = \Delta\epsilon_{00}(x_\parallel)$, we find that a matrix eigenvalue problem for $1/\Delta$ as a function of the impurity mode frequency can be developed and solved. Extension to non-linear dielectric impurities can be made by taking $\Delta = A(1 + \lambda|E|^2)$ and solving an eigenvalue problem for A. Extensions to frequency-dependent linear dielectric materials in which Δ is specified by some fixed form (i.e. $\Delta = \epsilon(\omega)$) can be solved graphically using the plots of the eigenvalues Δ as functions of ω and the plots of $\epsilon(\omega)$ as functions of ω to find the points where $\Delta = \epsilon(\omega)$.

For the cases studied in this paper we find:

(i) The delta function impurities for $n = 0$ modes yield single-valued functions in each symmetry mode for Δ as a function of impurity frequency.

(ii) Impurities with non-zero cross-sectional areas yield multiple-valued functions in each symmetry mode for Δ as a function of impurity frequency. As the cross-sectional area of the impurity increases, an increasing number of mode solutions accumulate near the lowest-valued Δ solution in the system. The increased number of Δ solutions for a fixed impurity mode frequency ω no doubt is associated with resonance effects due to the finite cross-sectional area of the impurity.

(iii) In general for $n = 0$, $|\Delta|$ is seen to be a decreasing function of impurity mode frequency. Exceptions to this are the s, s0 and s1 modes found in the lowest band gap of the system treated in this paper. For these modes an interesting asymptotic behaviour was observed in the case of the s mode in the dependence of Δ on ω, and the s0 and s1 modes exhibited a minimum and maximum, respectively, in their dependence of Δ on ω.

(iv) The values of Δ for $n = 0$ gap impurity modes tend to be smaller in gaps occurring at high frequencies than in those occurring at low frequencies.

(v) For $n = 1$ delta function single impurity modes, Δ is found to be a decreasing function of the impurity mode frequencies and those modes have three solutions of Δ for each impurity frequency corresponding to the possible electric field polarizations.

Owing to the small cross-sectional areas of the impurities considered in this paper, large values of impurity dielectric constants are needed to produce bound states in the gaps. Such large values can be found in materials with dielectric resonances. As the cross-sectional area of the impurity is found to increase, however, the impurity bound states are found to occur for impurities with smaller dielectric constants. Currently computational efforts are under way to extend the results in this paper to treat impurities of greater cross-sectional area.

Finally, we point out that current interest in impurity modes in photonic band structures resides in their use as high-Q electromagnetic cavities [6, 10]. The mode frequencies of these high-Q cavities can be extended to high frequency ranges in which existing superconducting cavity technology fails due to energy losses. Aside from their use as high-Q resonators, suggestions have been made for the use of impurity modes in the design of single-mode light-emitting diodes (SM-LED) and the possible development of such structures, which would

exhibit zero-threshold lasing [6]. (A good summary of these applications is given in the conference summary 'Development and applications of materials exhibiting photonic band gaps' of Bowden *et al* [22] and the subsequently published papers of the same conference.) It is for these reasons that we hope that our methodology, introduced above, will facilitate the study of impurity modes in photonic band structures. Aside from the methodology we have also exhibited how: (i) optically non-linear impurities can be used to tune resonance modes (and possibly tune lasers created from them), and (ii) clusters of impurities can be used to create a series of high-Q resonance levels, which can be designed to have very specific frequency intervals between them.

Up till now most theoretical efforts on impurity modes in photonic band structures have concentrated on 3D systems [6], with some initial efforts on the theoretical [8] and experimental [13, 23] study of 2D systems. The 2D systems experimentally studied to date have dealt only with a limited number of impurity geometries and values of the impurity dielectric constant that require considerable computer CPU time to study theoretically (even by the methods proposed here) and hence preclude general studies of the dependence of mode frequency on the impurity dielectric constants as presented in this paper. We hope that the results for the 2D impurity geometries evaluated in this paper will encourage further experiments along the lines suggested by our results.

Acknowledgment

This work is supported in part by NSF grant DMR 92-13793.

References

[1] Yablonovitch E 1987 *Phys. Rev. Lett.* **58** 2059
[2] John S 1987 *Phys. Rev. Lett.* **58** 2486
[3] Ho K M, Chan C T and Sonkonlis C M 1990 *Phys. Rev. Lett.* **65** 3152
[4] Plehal M, Shambrook A, Maradudin A A and Sheng P 1991 *Opt. Commun.* **80** 199
[5] Meade R D, Brommer K D, Rappe A M and Joannopoulos J D 1992 *Appl. Phys. Lett.* **61** 495
[6] Yablonovitch E 1993 *J. Opt. Soc. Am.* B **10** 283
[7] Yeh P 1988 *Optical Waves in Layered Media* (New York: Wiley)
[8] McGurn A R and Maradudin A A 1993 *Phys. Rev.* B **48** 17576
[9] Pendry J B, MacKinnon A and Roberts P J 1992 *Proc. R. Soc.* A **437** 67
[10] Yablonovitch E, Gmitter T J, Meade R D, Rappe A M, Brommer K D and Joannopoulos J D 1991 *Phys. Rev. Lett.* **67** 3380
[11] Maradudin A A and McGurn A R 1993 *Photonic Band Gaps and Localization* ed C M Soukoulis (New York: Plenum) p 247
[12] Leung K M 1993 *J. Opt. Soc. Am.* B **10** 303
Sigalas M, Sonkonlis C M, Economow E N, Chan C T and Ho K M 1993 *Phys. Rev.* B **48** 14 121
[13] Smith D R, Dalichaouch R, Kroll N, Schultz S, McCall S L and Platzman P M 1993 *J. Opt. Soc. Am.* B **10** 314
[14] Stanley R P, Houdre R, Oestrele U and Slegem M 1993 *Phys. Rev.* A **48** 2246
[15] Maradudin A A and McGurn A R 1993 *J. Opt. Soc. Am.* B **10** 307
[16] Maradudin A A and McGurn A R 1994 *J. Mod. Opt.* **41** 275
[17] Izyumov I A 1970 *Magnetic Neutron Diffraction* (New York: Plenum)
[18] Izyumov I A 1973 *Magnetically Ordered Crystals Containing Impurities* (New York: Consultants Bureau)
[19] Elliott R J, Krumhansl J A and Leath P L 1974 *Rev. Mod. Phys.* **46** 465
[20] Callaway J 1964 *Energy Band Theory* (New York: Academic)
[21] McGurn A R and Tahir-Kheli R A 1978 *Phys. Rev.* B **17** 2316
[22] Bowden C M, Dowling J P and Everitt H O 1993 *J. Opt. Soc. Am.* B **10** 280
[23] McCall S L, Platzman P M, Dalichaouch R, Smith D and Schultz S 1991 *Phys. Rev. Lett.* **67** 2017